PHYSICAL REVIEW E **77**, 020702(R) (2008)

Inhomogeneous bulk nematic order reconstruction

G. Lombardo,[1] H. Ayeb,[1] F. Ciuchi,[1] M. P. De Santo,[1] R. Barberi,[1,*] R. Bartolino,[1] E. G. Virga,[2] and G. E. Durand[3]
[1]*CNR-INFM LiCryL, Cemif.Cal, Physics Department, University of Calabria, 87036 Rende, Italy*
[2]*Dipartimento di Matematica, INFM-CNISM, Università di Pavia, via Ferrata 1, 27100 Pavia, Italy*
[3]*Laboratoire de Physique des Solides associé au CNRS, Université Paris Sud, 91405 Orsay, France*
(Received 17 October 2006; revised manuscript received 4 November 2007; published 20 February 2008)

A two-dimensional model within the $\bar{\bar{Q}}$-tensor description of liquid crystals is used to describe the inhomogeneous order reconstruction in a nematic cell driven by tony modulation in the anchoring conditions. Homogeneous and inhomogeneous reconstruction are contrasted: the former is defectless, the latter is defect mediated. While the transition thresholds are comparable in both cases and in good agreement with experimental data, the biaxial wall breaking is considerably slower in the inhomogeneous transition than in the homogeneous one. The shape of the signal given by the electric current flowing through the cell allows us to distinguish the actual path followed by the transition.

DOI: 10.1103/PhysRevE.77.020702 PACS number(s): 64.70.M−, 61.30.Gd

During the last four years, the research in nematic electro-optics has been strongly stimulated by the demonstration of fast coherent switching between two topologically distinct textures by means of the electrically controlled biaxial order reconstruction in nematics (BORN) [1]. Thermotropic nematics consist of rigid molecular core units, which are usually represented by physicists as simple rods, with a cylindrical symmetry. These calamitic units can build a nematic phase with uniaxial order. For this reason, usually nematic materials are described by using the scalar order parameter S and the director $\mathbf{n}$. $\mathbf{n}$ indicates the average molecular orientation and S the degree of order [2]. Nevertheless, uniaxial nematics under strong external constraints can induce a local and/or transient biaxial order at nanometric scale and the $(\mathbf{n},S)$ description is no longer adequate. This is the case of BORN, which requires a tensorial description of the nematic material.

The BORN allows the dynamical reconstruction of the long axis of the nematic order tensor $\bar{\bar{Q}}$ in a perpendicular direction with respect to a starting one. This means that a nematic texture can locally be reconstructed in a perpendicular direction without any rotation of $\mathbf{n}$. This allows us to connect nematic textures with different topologies as in the case of the π cell, where a slightly splayed texture is transformed in a bent one by means of a transient thin biaxial wall in the nematic bulk [1,3]. The BORN behavior in the π cell has been recently described by using a one-dimensional dynamical Landau–de Gennes–Khalatnikov model [1]. Moreover, the BORN time resolved experimental analysis has been presented by using electric current measurements coupled with texture transformation optical observations [4].

By looking at all the recent reports [1,3–6] on BORN, two main questions remain quite intriguing: discrepancies exist among the more advanced quantitative theoretical model proposed up to now [1] and all known experimental data; the current peak associated to the biaxial wall breaking is not always clearly detected in all experiments when the splay-bend transition takes place in the π cell. In this Rapid Communication, we address these two problems, using an improved two-dimensional $\bar{\bar{Q}}$ tensor model, whose complete description has just been submitted for publication [7].

The liquid crystal orientation and order are well described by a second rank tensor order parameter $\bar{\bar{Q}}$ and its dynamics is governed by a balance between the dissipation and the free energy variation [2,8]. For electro-optical experiments, by considering only the interaction with a quasistatic electric field, the total free energy is built by considering the distortion elastic energy of the nematic texture, the electric energy due to the interaction of the nematic structure with the external electric field, the thermotropic energy that dictates the preferred thermodynamical state of the nematic material, and the surface energy due to the interaction between the boundary surface and the nematic. In this work, we solve two-dimensional cases, adding to the elastic energy third order terms in the Landau representation to remove the degeneracy between splay and bend elastic constants [7]. Moreover, the temperature dependence of the coefficients of the elastic constants expressions is taken into account and the scalar order parameter is evaluated by calculating the minimum of the Landau–de Gennes potential [1,2]. Ions effects are neglected, and the nematic is considered as a pure dielectric material.

To solve the governing equations, we use a numerical method, using a finite element approach with a mesh size that can decrease down to 5 nm. Starting from the $\bar{\bar{Q}}$ evolution, we can calculate the temporal behavior (with a maximum time step of 0.1 μs) of the electric potential, of the scalar order parameter, of the biaxiality, and of the director orientation in each point of the mesh [7]. Moreover, the electric current density that flows through the cell is evaluated for a direct comparison with dynamical experimental observations [1,4].

The experimental data are obtained using the same experimental setup and methods already described in [1,4,6]. A typical sample is a sandwich planar cell with two flat glass plates, coated by a transparent indium tin oxide (ITO) film, which are glued together to be spaced about 2 μm. The cell is filled with 4-cyano-4′-**n**-pentylbiphenyl, brand K15 from Merck (also known as 5CB), in a vacuum chamber at 40 °C. The ITO film is treated by photolithography to obtain a pixel

*Corresponding author; barberi@fis.unical.it

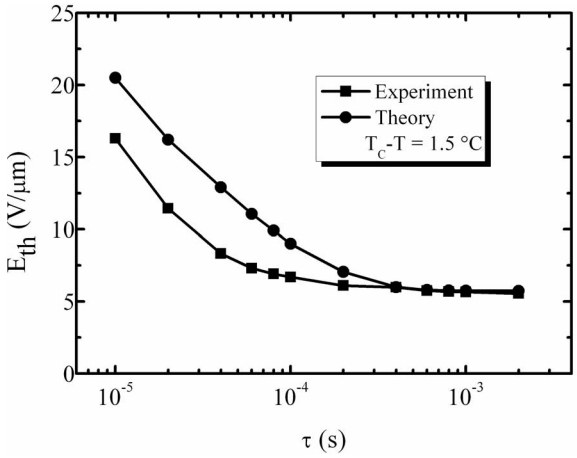

FIG. 1. Comparison between theoretical data produced by the numerical model and experimental data for the electric BORN threshold E_{th} for 5CB at $T=T_c-1.5$ °C, for different electric pulse lengths τ in the range from 0.01 to 2 ms.

of about 1 mm^2 area. The cell spacers are mixed with the glue, which is deposited outside the pixel area, to avoid wall breaking by defects around spacers and the anchoring treatments have been chosen to match the best recent behavior reported in literature, with the highest possible electric threshold for the BORN [5,6].

The π cell has been observed by using a polarizing optical microscopy and its temperature has been controlled within 0.1 °C by a heating stage. Square electric pulses of amplitude E_{th} and length τ are applied perpendicularly to the plates of the sandwich cell to obtain the BORN effect, when the starting splay texture is transformed in a bent one by the external electric field.

Figure 1 shows the experimental electric threshold data E_{th} compared with the numerical results obtained by the model at $T=(T_c-1.5)$ °C, where T_c is the clearing point of the nematic. We compare experiments made by using a sample with aligning surface layers with a 20% polyamic acid (LQ1800 by Hitachi Chemical) concentration in 1-methyl-2-pyrrolidinone and an ideal numerical case, having an 8° pretilt with infinite anchoring energy strength on both boundary surfaces. The LQ1800 aligning layers give a strong anchoring strength $W=2.5\times10^{-4}$ J/m^2, measured by optical retardation vs applied voltage [9], and induce on the nematic a pretilt angle of about 8°, measured by means of a standard interferential method [10].

For a better comparison, one has to take into account that the aligning layer has a finite thickness in order to evaluate the actual electric field acting on the nematic layer. A typical cell of total thickness d is in fact composed by three layers: two boundary polymeric layers of thickness d_P and the main liquid crystal layer of $d-2d_P$ thickness, having different average dielectric constants: ϵ_P for the LQ1800 layers and ϵ_{LC} for the nematic layer. By applying the continuity of the normal component of the dielectric vector through the cell and calling $\mathbf{E}$ the applied electric field, we obtain the actual electric field $\mathbf{E}_{LC}$ acting on the liquid crystal: $E_{LC}/E=d/[(d-2d_P)+2(\epsilon_{LC}/\epsilon_P)d_P]$. The LQ1800 aligning layers average thicknesses have been measured both by an ellipsometric method and by x-ray reflectometry, with comparable results: (50 ± 3) nm. Using the previous equation, the maximum electric drop in our samples is in percentage 18%.

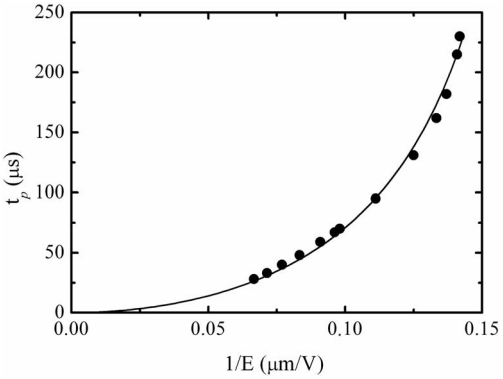

FIG. 2. BORN electric peak delay t_p for electric fields larger than the threshold value E_{th}. Circles represent data obtained by our numerical model and the continuous line is a best fit using the phenomenological law proposed in [4].

Figure 1 shows a good agreement between theory and experiments near the nematic-isotropic transition for electric pulse lengths ranging from 0.1 to 1 ms, strongly improving the results of Ref. [1]. The discrepancies for electric pulses shorter than 0.1 ms could be solved by a better hydrodynamical description.

The numerical model has also been tested to simulate the temporal positions of the BORN electric peak for electric fields larger than the threshold value E_{th}. These results are reported in Fig. 2, where the peak temporal delays t_p, measured with respect to the starting time $t=0$ when the electric field is switched on, are plotted vs $1/E$. These numerical data are well fitted by the phenomenological law $1/t_p=(1/t_{th})(E^2-E_{th}^2)/E_{th}^2$ proposed in [4], obtaining a further confirmation of a good agreement between the theoretical model and the experimental observations. t_{th} is the characteristic transition time given by the wall thinning time and the full order reconstruction time [5,6].

As stated in all the previously reported experiments [1,3–5], at first glance, one does not expect any effect coming from surface treatments because, close to the biaxial transition, the electric coherence length is very short, much shorter than the cell thickness. Therefore, starting from a perfectly uniform and symmetric splayed state, just below the threshold for the biaxial melting, the nematic texture becomes homeotropic everywhere, except in three thin layers: the biaxial wall, in the middle of the cell, and two regions, close to the boundary surfaces. The thicknesses of these three layers are in all cases comparable with the electric coherence length itself. Therefore the bulk biaxial wall and the alignment layers should be decoupled by the two intermediate, highly ordered, homeotropic textures, which connect the biaxial wall with the upper and the lower anchoring regions.

The analysis of the biaxial transition is usually made by implicitly considering the case of a uniform wall, perfectly parallel to the planar boundary plates. This is a limit case which implies that the boundary physical parameters are perfectly uniform everywhere. This approach allowed us to use

a simplified one-dimensional description for the first dynamical numerical model [1]. If we admit that the biaxial wall could, for instance, undulate, the switching mechanism could be affected by this phenomenon. Recently, for instance, a two-dimensional dynamical model suggests that small undulation of the biaxial wall could allow transitions through defect nucleation and disclination line movement [11]. The theoretical frame of this model has not been completely explained by the authors, and the wall undulation is produced by using as initial condition a sinusoidal numerical perturbation in the middle of the cell. As an undulation of the biaxial wall could be generated by surface inhomogeneities, and in a real cell it is very difficult to obtain a complete homogenous surface treatment, surface parameters must be investigated. Surface inhomogeneities can be, for instance, related to local variations of the pretilt angle and/or to local variations of the anchoring energy and/or with local variation of the aligning film thickness [12] and/or local variations of the surface order [13].

To theoretically investigate the hypothesis of inhomogeneous surface treatments, we analyze the time evolution of $\bar{\bar{Q}}$ on vertical rectangular sections representing two ideal samples: the first one C_1 with a full symmetric situation and perfectly homogeneous boundary conditions on the horizontal plates, with a pretilt of 1°, which produce a perfect splayed texture, and the second one C_2, whose boundary conditions on the planar plates simulate a small surface inhomogeneity. In the case of C_2, the anchoring conditions are periodic and the pretilt slowly varies with a sinusoidal modulation of $1°+0.5°\sin(2\pi x/\lambda)$ for the lower surface and $-1°+0.5°\sin(2\pi x/\lambda+\phi)$ for the upper substrate. By varying λ or ϕ, we numerically control the cell inhomogeneity. In the following example of case C_2, we fix $\lambda=2$ μm and $\phi=\pi/4$, values which give the highest perturbation in the middle of the cell. In both cases, C_1 and C_2, we assume an infinite anchoring energy. All calculations are performed by using periodic conditions on the vertical boundaries.

In the case C_1, when the applied field is strong enough to exceed the electric BORN transition threshold, the biaxial wall is parallel to the boundary plates and it vanishes uniformly. The wall is completely broken at $t=85$ μs, when the sample orientation in the bulk of the nematic is almost homeotropic everywhere. By looking in Fig. 4 at the calculated electric current (full circles) flowing through the nematic material, we observe the formation of two well defined peaks, the fastest and largest one due to the dielectric realignment toward the homeotropic orientation of the two layers around the biaxial wall and the second one due to the biaxial wall breaking.

In the case of the C_2 configuration, the second electric peak, related to the BORN, practically does not exist any more, substituted by a larger and shorter irregular structure, wider in time and shorter in amplitude (empty circles of Fig. 4), due to the fact that now the biaxial wall undulates and does not disappear everywhere at the same time as shown in Figs. 3(a)–3(c). In these pictures, the local director orientation is mapped linearly from white, which represents the homeotropic orientation, to black, which represents the planar orientation. In the case C_2, one observes a defect-mediated

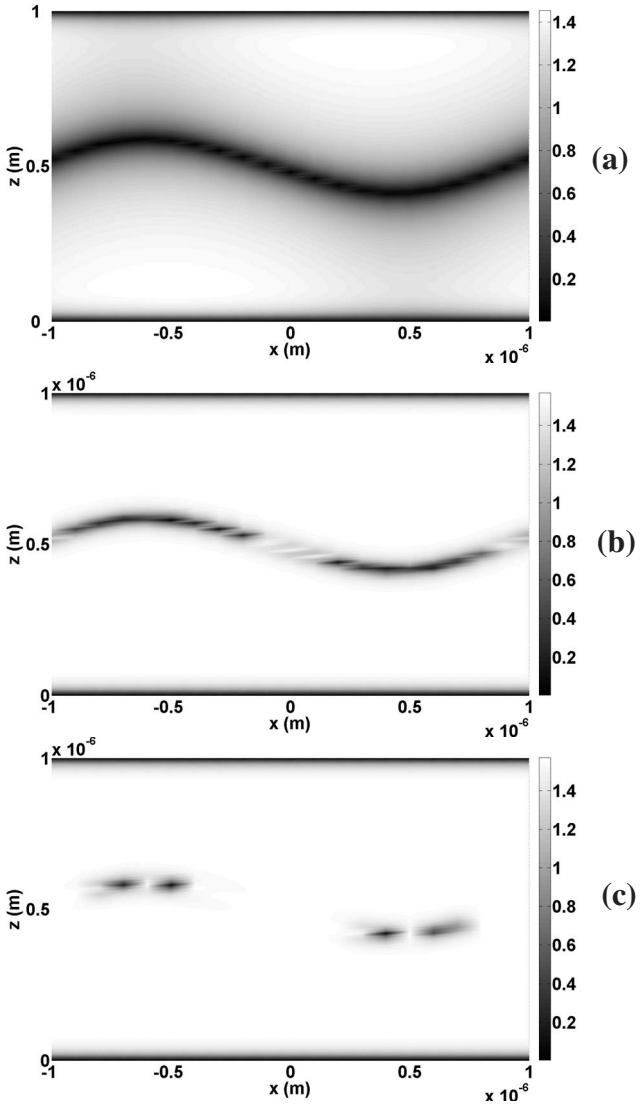

FIG. 3. Calculated time evolution of the biaxial wall in the case of inhomogeneous defects-mediated BORN. Each picture represents a vertical section of the sample. The local director orientation is mapped linearly from white, which represents the homeotropic orientation, to black, which represents the planar orientation. Each picture represents a snapshot at a time t after the starting of the electric pulse: t is 50 μs for (a), 85 μs for (b), 100 μs for (c).

wall breaking. The practical suggestions of [5], to not put spacers in the active pixel area and to reduce the pixel area itself, are hence not sufficient to avoid this effect. In principle, even a weak distortion at the surface can give rise to a nonhomogeneous breaking of the wall and, as the electric current observation is highly sensitive to this phenomenon, it can be used to detect and to distinguish uniform or inhomogeneous bulk nematic order reconstructions. Both cases have been widely observed in our experiments.

In the uniform case of the C_1 configuration, the biaxial wall has disappeared after 85 μs since the electric pulse application, while Figs. 3(b) and 3(c) show that the defects evolution in the inhomogeneous case is not completed after 100 μs. In the uniform case, the width of the BORN electric peak is quite short (5 μs), while the electric response in the

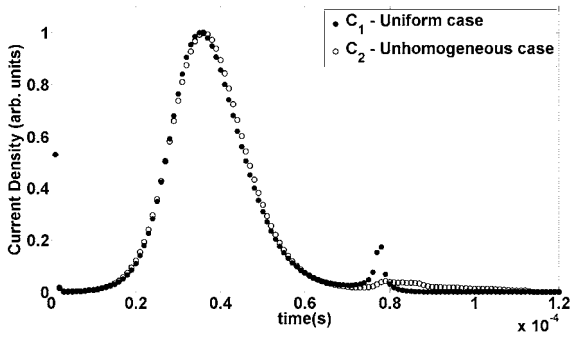

FIG. 4. Numerical evaluation of the electric current flowing through the cell vs time in the case of uniform (full circles) and in the case of inhomogeneous defects-mediated BORN (empty circles).

inhomogeneous case extends on a larger time interval (30 μs) as shown in Fig. 4. In the uniform case, the energy of the biaxial wall is released everywhere in a short time, building a well defined electric peak, while in the inhomogeneous case, the energy is released first by forming couples of defects and then annealing them on a longer time scale, with a resulting electric signal without a well defined shape. Therefore the uniform wall disappearing is faster than the defect mediated wall breaking, in contrast with conclusions of Ref. [11]. We also emphasize that a small surface perturbation produces a wide undulation of the biaxial wall, whereas the artificial undulations reported in Ref. [11] have a much smaller scale, probably due to quenching by the uniform boundary conditions. Our investigations with very small surface pretilt show that the uniform and inhomogeneous transition mechanisms present practically the same threshold. Only the boundary conditions determine which transition will take place, and the actual path of the BORN can be easily checked by electric current observations.

The authors acknowledge support from MIUR, project PRIN2004 n.2004024508, and from CNR, project LiCryL-MD.P10.009. The authors also acknowledge A. Pane and O. Pizzino for technical support in the clean room and for cells preparation, A. Mazzulla and M. Giocondo for x-ray measurements, and S. D'Elia for ellipsometric measurements.

[1] R. Barberi, F. Ciuchi, G. Durand, M. Iovane, D. Sikharulidze, A. Sonnet, and E. Virga, Eur. Phys. J. E **13**, 61 (2004).
[2] P. G. de Gennes and J. Prost, in *The Physics Liquid Crystals* (Clarendon, Oxford, 1993).
[3] P. Martinot-Lagarde, H. Dreyfus-Lambez, and I. Dozov, Phys. Rev. E **67**, 051710 (2003).
[4] R. Barberi, F. Ciuchi, G. Lombardo, R. Bartolino, and G. Durand, Phys. Rev. Lett. **93**, 137801 (2004).
[5] S. Joly, I. Dozov, and P. Martinot-Lagarde, Phys. Rev. Lett. **96**, 019801 (2006).
[6] R. Barberi, F. Ciuchi, H. Ayeb, G. Lombardo, R. Bartolino, and G. Durand, Phys. Rev. Lett. **96**, 019802 (2006).
[7] G. Lombardo, H. Ayeb, and R. Barberi (unpublished).
[8] A. M. Sonnet and E. G. Virga, Phys. Rev. E **64**, 031705 (2001).
[9] S. Palto, R. Barberi, M. Iovane, V. Lazarev, and L. Blinov, Mol. Mater. **11**, 277 (1999).
[10] H. A. Van Sprang, Mol. Cryst. Liq. Cryst. **199**, 19 (1991).
[11] Y. Zhang, D. B. Chung, B. Wang, P. J. Bos, Liq. Cryst. **34**, 143 (2007).
[12] A. Alexe-Ionescu, R. Barberi, G. Barbero, J. Bonvent, and M. Giocondo, Appl. Phys. A: Mater. Sci. Process. **61**, 425 (1995).
[13] R. Barberi and G. Durand, Phys. Rev. A **41**, 2207 (1990); R. Barberi, M. Giocondo, J. Li, R. Bartolino, I. Dozov, and G. Durand, Appl. Phys. Lett. **71**, 3495 (1997).